Optimal Reaction Conditions for the Minimization of Energy Consumption and By-Product Formation in a Poly(ethylene terephthalate) Process

Kyoung-Su Ha, Hyun-Ku Rhee

School of Chemical Engineering and Institute of Chemical Processes, Seoul National University, Kwanak-ku, Seoul 151-742, Korea

Received 15 December 2001; accepted 24 January 2002

ABSTRACT: We determined the optimal reaction conditions to minimize the energy cost and the quantities of by-products for a poly(ethylene terephthalate) process by using the iterative dynamic programming (IDP) algorithm. Here, we employed a sequence of three reactor models: the semibatch transesterification reactor model, the semibatch prepolymerization reactor model, and the rotating-disc-type polycondensation reactor model. We selectively chose or developed the reactor models by incorporating experimentally verified kinetic models reported in the literature. We established the model for the entire reactor system by connecting the three reactor models in series and by resolving some joint problems arising when different types of reactor models were interconnected. On the basis of the simulation results of the reactor system, we scrutinized the cause and effect between the reaction conditions and the final quality of the polymer product. Here, we set up the optimization strategy by using IDP on the basis of the integrated reactor model, and the process variables with significant influence on the properties of polymer were selected as control variables with the help of a simulation study. With this method, we could refine the reaction conditions at the end of each iteration step by contracting the spectra of control regions, and the iteration process finally stopped when the profile of the optimal trajectory converged. We also took the constraints on the control variables into account to guarantee polymer quality and to suppress side reactions. Constituting six different strategies by setting weighting vectors differently, we examined the differences in optimal trajectories, the trend of optimality, and the quality of the final polymer product. For each of the strategies, we conducted the optimization to examine whether the number-average degree of polymerization approached the desired value. © 2002 Wiley Periodicals, Inc. J Appl Polym Sci 86: 993–1008, 2002

Key words: polycondensation; poly(ethylene terephthalate); simulations; optimization; iterative dynamic programming; constraint

INTRODUCTION

In recent years, there have been many reports on modeling poly(ethylene terephthalate) (PET) polymerization kinetics and reactor systems. Among them, Ravindranath and Mashelkar[1–4] studied the modeling of each stage in the PET process and suggested that someone model the reactors with functional group analysis. On the other hand, Lei and Choi[5,6] applied the molecular species model and the moment equation method for the process. Many preceding works rigorously disclosed the kinetics of the melt polymerization of PET. The review articles by Ravindranath and Mashelkar[4,7] provided excellent surveys to elaborate the reaction kinetics and the kinetic model.

From these works, we noticed that the PET polymerization of industrial practice is more complex than one may expect. A multitude of polymerization reaction pathways, such as propagation, degradation, and side reactions, offers many challenging problems for the regulation of polymer quality. For example, a small amount of diethylene glycol (DEG) lowers the melting point and the thermal stability of PET. A few parts per million acetaldehyde gives an odor to PET bottles and brings about coloring problems Carboxyl end groups, hydroxyl end groups, methyl end groups, vinyl end groups, cyclic oligomers, and water are also known to affect the polymer quality. Thus, it is very important to establish an optimization scheme to regulate such undesired side products. Unfortunately, however, works on the optimization or control of the process are rather scarce. Those that exist have concentrated on a specific stage of the entire process. Therefore, we were motivated to find the optimized reaction conditions that would minimize simultaneously the energy consumption and the formation of by-products.

We are now in a position to introduce our control scheme. To obtain the best policy, many researchers have devised various algorithms for polymerization reactor systems, taking into consideration highly nonlinear features and input constraints. Among the non-

Correspondence to: H.-K. Rhee (hkrhee@snu.ac.kr).

Contract grant sponsor: Brain Korea 21 Program, supported by the Ministry of Education.

Journal of Applied Polymer Science, Vol. 86, 993–1008 (2002)

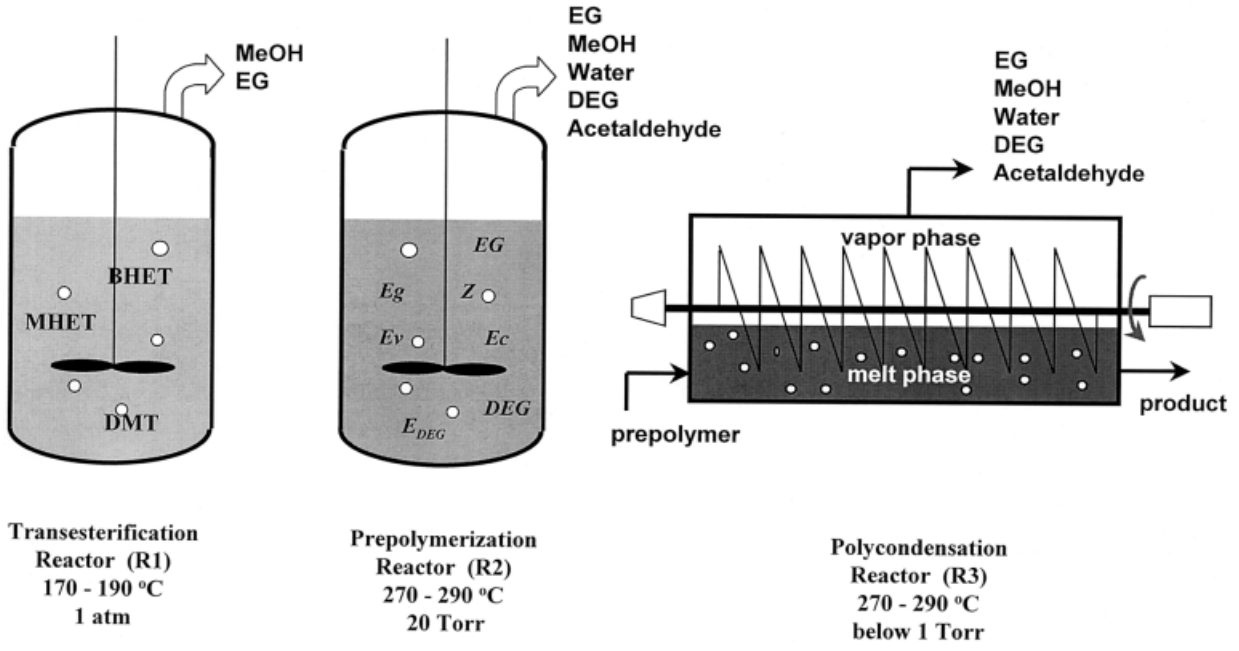

Figure 1 Schematic diagram of the three different stages for the entire PET process.

linear control methodologies, optimization and transformation methods fall into two main categories. Most of the approaches based on the transformation or the Jacobian (partial or full) linearization have the advantage of well-developed theoretical analysis for stability and robustness. It is, however, well known that the linear control theory based on the transformation method cannot properly deal with the characteristics of highly nonlinear processes such as polymerization reactor systems. These approaches are often limited to certain classes of nonlinear systems and can generate physically unrealizable state variables, for instance, mole fractions greater than unity.[8] Therefore, an optimization method capable of finding the global optimum despite the difficulty in handling highly nonlinear dynamics of the polymerization reactor is in demand. In addition, to reduce the cost of operation and to obtain the desired polymer properties, a scheme to optimize the concerned reaction conditions is indeed required within an allowable control region. Of many optimization techniques, iterative dynamic programming (IDP), which is well known to have a strong possibility for finding the global optimum and which easily incorporates constraints on control variables and states,[9] was thought to be an excellent choice for the system of our concern.

Pet polymerization process

For the modeling of the PET process, we took into account the three consecutive reactors: a semibatch transesterification reactor, a semibatch prepolymeriza-

TABLE I
Chemical Formulae of Polymeric Species Considered in the Transesterification Reactor

P_n	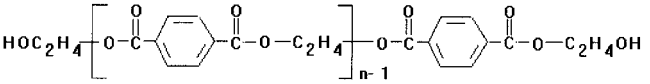
Q_n	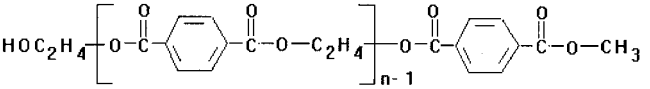
R_n	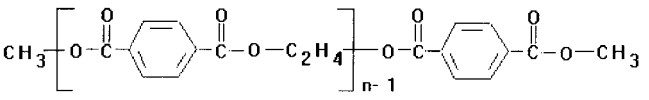

All the symbols in the table also denote their respective numbers of moles in eqs. (10–14).

TABLE II
Main Reactions Considered in the Transesterification Reactor

1. Ester interchange reaction

$$R_n + G \underset{k_i'}{\overset{k_i}{\rightleftarrows}} Q_n + M \quad (1)$$

$$Q_n + G \underset{k_i'}{\overset{k_i}{\rightleftarrows}} P_n + M \quad (2)$$

2. Polycondensation reaction:

$$P_n + P_m \underset{k_p'}{\overset{k_p}{\rightleftarrows}} P_{n+m} + G \quad (3)$$

$$P_n + Q_m \underset{k_p'}{\overset{k_p}{\rightleftarrows}} Q_{n+m} + G \quad (4)$$

$$Q_n + Q_m \underset{k_p'}{\overset{k_p}{\rightleftarrows}} R_{n+m} + G \quad (5)$$

3. Transesterification reaction:

$$P_n + R_m \underset{k_t'}{\overset{k_t}{\rightleftarrows}} Q_{n+m} + M \quad (6)$$

$$P_n + Q_m \underset{k_t'}{\overset{k_t}{\rightleftarrows}} P_{n+m} + M \quad (7)$$

$$Q_n + Q_m \underset{k_t'}{\overset{k_t}{\rightleftarrows}} Q_{n+m} + M \quad (8)$$

$$Q_n + R_m \underset{k_t'}{\overset{k_t}{\rightleftarrows}} R_{n+m} + M \quad (9)$$

tion reactor, and a rotating-disc-type polycondensation reactor. There are two different methods that are usually adopted for the kinetic modeling of the PET process. One can use the simpler approach of functional group modeling, in which only the reactions between the reactive functional groups are considered. The other approach is concerned with molecular species modeling, in which every component in the reaction mixture is treated as an independent chemical entity. For the simulation of the transesterification reactor, the molecular species model[5] was used together with the method of moment. Although a detailed molecular species model can give a complete product composition distribution and molecular-weight distributions of various polymeric species, it certainly suffers from a heavy computational requirement. Such a detailed model may not be suitable for the subsequent two reactors because complicated side reactions should be considered under more severe reaction conditions in addition to ester interchange, transesterification, and polycondensation reactions. In this study, therefore, we adopted the functional group modeling approach[2,10] for the simulation of the prepolymerization reactor and the polycondensation reactor.

Figure 1 shows the schematic diagram of the entire PET process. Each reactor was operated under isothermal and isobaric conditions. In the first stage of the PET polymerization process, in the transesterification reactor with zinc acetate as the catalyst, functional groups of dimethyl terephthalate (DMT) and ethylene glycol (EG) reacted to yield bis(2-hydroxyethyl) terephthalate (BHET), various oligomers, and the condensate, methanol (MeOH), which needed to be removed. The feed molar ratio of DMT to EG was set equal to 2 so that both the ends of the DMT molecules could be capped with EG after the elimination of MeOH. The main product, BHET, served as the monomer in the second stage. Three kinds of oligomers could be identified by their functional end groups,[6] and their chemical formulae are shown in Table I.

Considering the reactions listed in Table II, one can formulate the mass balance equations for the transesterification reactor as follows:

$$\frac{dP_n}{dt} = \frac{1}{V}\Bigg\{ 2k_iQ_nG - 2k_i'P_nM - 2(n-1) \times P_n(k_t'M + 2k_p'G) - 2P_n \sum_{m=1}^{\infty} [k_t(Q_m + 2R_m) + k_p(2P_m + Q_m)] + (k_t'M + 2k_p'G) \sum_{m=n+1}^{\infty} (2P_m + Q_m) + 2\sum_{r=1}^{n-1} (k_tP_rQ_{n-r} + k_pP_rP_{n-r}) \Bigg\} \quad (10)$$

$$\frac{dQ_n}{dt} = \frac{1}{V}\Bigg\{ 2k_iG(2R_n - Q_n) + k_i'M(2P_n - Q_n) - 2(n-1)Q_n(k_t'M + 2k_p'G) - Q_n \sum_{m=1}^{\infty} [2k_t(P_m + Q_m + R_m) + k_p(2P_m + Q_m)] + 2\sum_{m=n+1}^{\infty} [k_t'M(P_m + Q_m + R_m) + k_p'G(Q_m + 2R_m)] + \sum_{r=1}^{n-1} [k_t(Q_rQ_{n-r} + 4P_rR_{n-r}) + 2k_pP_rQ_{n-r}] \Bigg\} \quad (11)$$

$$\frac{dR_n}{dt} = \frac{1}{V}\Bigg[-4k_iR_nG + k_i'Q_nM - 2(n-1)R_n(k_t'M + 2k_p'G) - 2k_iR_n \sum_{m=1}^{\infty} (2P_m + Q_m) + k_t'M \sum_{m=n+1}^{\infty} (Q_m + 2R_m) + \sum_{r=1}^{n-1} (2k_tQ_rR_{n-r} + 0.5k_pQ_rQ_{n-r}) \Bigg] \quad (12)$$

TABLE III
Functional Groups and By-Product Species Considered in the Prepolymerization and Melt Polycondensation Reactors

Symbol[a]	Functional group	Symbol[a]	Condensate
Z	Diester group	EG	Ethylene glycol
E_g	Hydroxyl group	DEG	Diethylene glycol
E_c	Carboxylic acid group	W	Water
E_{DEG}	DEG end group	A	Acetaldehyde
E_v	Unsaturated vinyl group	M	Methanol
E_m	Methyl ester group		

[a] All the symbols in the table also denote their respective concentrations in eqs. (26–58).

$$\frac{dM}{dt} = \frac{1}{V}\left\{\sum_{n=1}^{\infty}[2k_iG(Q_n + 2R_n) - k_i'M(2P_n + Q_n) + 2k_t'M(n-1)(P_n + Q_n + R_n)] + k_t\sum_{n=1}^{\infty}(2P_n + Q_n)\sum_{m=1}^{\infty}(Q_m + 2R_m)\right\} \quad (13)$$

$$\frac{dG}{dt} = \frac{1}{V}\left\{\sum_{n=1}^{\infty}[-2k_iG(Q_n + 2R_n) + k_i'M(2P_n + Q_n) - 4k_p'G(n-1)(P_n + Q_n + R_n)] + k_p\sum_{n=1}^{\infty}\left[4P_n\sum_{m=1}^{\infty}(P_m + 0.5Q_m) + Q_n\sum_{m=1}^{\infty}Q_m\right]\right\} \quad (14)$$

in which M and G represent the numbers of moles of MeOH and EG, respectively, and V denotes the volume of the reaction mixture. Then, one can develop the rate equations for the moments of polymer by using the method of moments. In this study, we used the equations for moments reported by Lei and Choi.[6] For each of the living and dead polymers, we set up balance equations for the zero, first, and second moments of the number of moles of polymer and adopted the moment closure technique for the third moment.[11] The number-average degree of polymerization (X_n) could be determined as follows:

$$X_n = \frac{\sum_{\xi}\lambda_{\xi,1}}{\sum_{\xi}\lambda_{\xi,0}} \quad (15)$$

where $\lambda_{\xi,i}$ is the ith moment of the number of moles of polymer and ξ is the type of polymeric species. Under reaction conditions of 170–190°C and ambient pressure, condensates such as MeOH and EG would vaporize to the vapor phase according to the vapor–liquid equilibrium. The ideal gas law was assumed to apply for the vapor phase, whereas Raoult's law was valid in the liquid phase.

The product stream from the transesterification reactor, which consisted mainly of BHET, was fed to the second semibatch reactor, called the prepolymerization reactor. Here, the reaction conditions were different from those of the first one, and Sb_2O_3 (0.025 wt %) was used as the catalyst. To produce a prepolymer with a chain length of 10–20, we kept the temperature higher (270–290°C) and the pressure lower (20 Torr) than in the first reactor. Table III shows the functional groups and the condensate molecules associated with the second reactor. The major functional end groups present in the reaction mixture were the hydroxyl group, the carboxylic acid group, the DEG group, and the unsaturated vinyl group. During the course of the polymerization reaction, an extensive redistribution of these functional end groups occurred, and a quantitative description of the reaction kinetics became quite complex. In addition, volatile condensates such as EG, free DEG, water, acetaldehyde, and MeOH were also produced and evaporated to the vapor phase. Of the

TABLE IV
Reactions Considered in the Prepolymerization and Polycondensation Reactors

Ester interchange	$E_m + \mathrm{EG} \underset{k_1/K_1}{\overset{k_1}{\rightleftharpoons}} E_g + M$	(16)
Transesterification	$E_m + E_g \underset{k_2/K_2}{\overset{k_2}{\rightleftharpoons}} Z + M$	(17)
Polycondensation	$2E_g \underset{k_3/K_3}{\overset{k_3}{\rightleftharpoons}} Z + \mathrm{EG}$	(18)
Acetaldehyde formation	$E_g \overset{k_4}{\rightarrow} E_c + A$	(19)
	$E_v + E_g \overset{k_{10}}{\rightarrow} Z + A$	(20)
DEG formation	$E_g + \mathrm{EG} \overset{k_5}{\rightarrow} E_c + \mathrm{DEG}$	(21)
	$2E_g \overset{k_6}{\rightarrow} E_c + E_{DEG}$	(22)
Water formation	$E_c + \mathrm{EG} \underset{k_7/K_7}{\overset{k_7}{\rightleftharpoons}} E_g + W$	(23)
	$E_c + E_g \underset{k_8/K_8}{\overset{k_8}{\rightleftharpoons}} E_g + W$	(24)
Degradation of diester group	$Z \overset{k_9}{\rightarrow} E_c + E_v$	(25)

condensates, acetaldehyde and MeOH are so volatile that we could assume these species were removed from the reactor right after they formed, whereas the other condensates were transferred from the liquid mixture to the vapor phase according to the vapor–liquid equilibria. The vapor–liquid equilibrium compositions were computed with the Flory–Huggins model. Reactions considered in this model are listed in Table IV.[2,3] According to Table IV, we could develop the mass balance equations for the prepolymerization reactor as follows:

$$\frac{dE_g}{dt} = R_1 - R_2 - 2R_3 - R_4 - R_5 - 2R_6 + R_7 - R_8 - R_{10} \quad (26)$$

$$\frac{dZ}{dt} = R_2 + R_3 + R_8 - 2R_9 + R_{10} \quad (27)$$

$$\frac{dE_m}{dt} = -R_1 - R_2 \quad (28)$$

$$\frac{dE_{\mathrm{DEG}}}{dt} = R_6 \quad (29)$$

$$\frac{dE_v}{dt} = R_9 - R_{10} \quad (30)$$

$$\frac{dE_c}{dt} = R_4 + R_5 + R_6 - R_7 - R_8 + R_9 \quad (31)$$

$$\frac{dM}{dt} = R_1 + R_2 \quad (32)$$

$$\frac{dA}{dt} = R_4 + R_{10} \quad (33)$$

$$\frac{d\mathrm{EG}}{dt} = -R_1 + R_3 - R_5 - R_7 \quad (34)$$

$$\frac{d\mathrm{DEG}}{dt} = R_5 \quad (35)$$

$$\frac{dW}{dt} = R_7 + R_8 \quad (36)$$

where E_g, Z, E_m, E_{DEG}, E_v, E_c, M, A, EG, DEG, and W are defined in Table III. The rate expressions (R_i's) are given by

$$R_1 = k_1(2E_mEG - E_gM/K_1) \quad (37)$$

$$R_2 = k_2(E_mE_g - 2ZM/K_2) \quad (38)$$

$$R_3 = k_3(E_g^2 - 4ZEG/K_3) \quad (39)$$

$$R_4 = k_4E_g \quad (40)$$

$$R_5 = 2k_5E_gEG \quad (41)$$

$$R_6 = k_6E_g^2 \quad (42)$$

$$R_7 = k_7(2E_cEG - E_gW/K_7) \quad (43)$$

$$R_8 = k_8(E_cE_g - 2ZW/K_8) \quad (44)$$

$$R_9 = k_9Z \quad (45)$$

$$R_{10} = k_{10}E_gE_c \quad (46)$$

In this model, X_n may be determined as follows:

$$X_n = 1 + \frac{2Z}{E_g + E_m + E_c + E_v + E_{\mathrm{DEG}}} \quad (47)$$

For practical use, the chain length of PET should be in the range 80–100 or higher. The product from the second reactor needed to be further processed. For this, it was very important to remove the EG condensate efficiently because the polycondensation reaction is reversible. In the polycondensation reactor, the viscosity of polymer melt became rather high, and the rate of EG transfer from the polymer melt phase to the vapor phase could have controlled the net reaction rate and, thus, the chain length. Therefore, it was necessary to use a specially designed reactor to enhance the mass transfer rate.[4] In this study, a rotating-disk-type reactor was considered, which could be modeled as a plug flow reactor (PFR).[10] The forward reaction of polycondensation is accelerated if the pressure is kept low, and this brings about a much more effective removal of EG. The values of the mass transfer rate constants for the volatile species such as EG, free DEG, and water were set to 0.05 s^{-1}.[2,10,12] The reactions in Table IV were taken into consideration in this study. The vapor–liquid equilibrium compositions were computed with the Flory–Huggins model. The Sb_2O_3 catalyst (0.025 wt %) was considered for this finishing reactor as in the prepolymerization reactor. Considering Table IV, we developed the mass balance equations at steady state for the polycondensation reactor as follows:

$$\frac{1}{\theta}\frac{dE_g}{dz} = R_1 - R_2 - 2R_3 - R_4 - R_5 - 2R_6 + R_7 - R_8 - R_{10} \quad (48)$$

$$\frac{1}{\theta}\frac{dZ}{dz} = R_2 + R_3 + R_8 - 2R_9 + R_{10} \quad (49)$$

TABLE V
Kinetic Parameters for the Reactions in Table II

k_i	$2.42 \times 10^{14}\exp(-28{,}900/RT)$ [C*] L/mol min
k_i'	$1.71 \times 10^{14}\exp(-26{,}800/RT)$ [C*] L/mol min
k_t	$1.92 \times 10^{11}\exp(-23{,}100/RT)$ [C*] L/mol min
k_t'	$1.79 \times 10^{11}\exp(-21{,}000/RT)$ [C*] L/mol min
k_p	$2.90 \times 10^{8}\exp(-18{,}500/RT)$ [C*] L/mol min
k_p'	$3.82 \times 10^{8}\exp(-18{,}500/RT)$ [C*] L/mol min
Catalyst concentration ([C*])	1.5×10^{-3} mol/L

$R = 1.987$ cal/mol K.

$$\frac{1}{\theta}\frac{dE_m}{dz} = -R_1 - R_2 \tag{50}$$

$$\frac{1}{\theta}\frac{dE_{\mathrm{DEG}}}{dz} = R_6 \tag{51}$$

$$\frac{1}{\theta}\frac{dE_v}{dz} = R_9 - R_{10} \tag{52}$$

$$\frac{1}{\theta}\frac{dE_c}{dz} = R_4 + R_5 + R_6 - R_7 - R_8 + R_9 \tag{53}$$

$$\frac{1}{\theta}\frac{dM}{dz} = R_1 + R_2 \tag{54}$$

$$\frac{1}{\theta}\frac{dA}{dz} = R_4 + R_{10} \tag{55}$$

$$\frac{1}{\theta}\frac{d\mathrm{EG}}{dz} = -R_1 + R_3 - R_5 - R_7 - k_{L,\mathrm{EG}}a(\mathrm{EG} - \mathrm{EG}^*) \tag{56}$$

$$\frac{1}{\theta}\frac{d\mathrm{DEG}}{dz} = R_5 - k_{L,\mathrm{DEG}}a(\mathrm{DEG} - \mathrm{DEG}^*) \tag{57}$$

$$\frac{1}{\theta}\frac{dW}{dz} = R_7 + R_8 - k_{L,w}a(W - W^*) \tag{58}$$

where θ and z are the mean residence time and the dimensionless distance from the reactor inlet, respectively, and $k_{L,j}a$ and C_j^* denote the mass transfer coefficient and the equilibrium concentration of the volatile species j at the interface, respectively. X_n was determined by eq. (47). The kinetic parameters for the reactions in Tables II and IV are given in Tables V and VI, respectively.

OBJECTIVE FUNCTION AND IDP WITH CONSTRAINTS

The process variables mainly affecting the property of the final polymer product were chosen on the basis of the simulation study for the entire reactor system. These were the reaction temperatures (T_1 in the first reactor, T_2 in the second reactor, and T_3 in the third reactor) and the pressure in the third reactor (P_3), and these are referred to here as the control variables. In the first or the second reactor, there was only one control variable, the reaction temperature, but the third reactor had two control variables, the temperature and the pressure. We included both P_3 and T_3 in the control variables because the mass transfer rates of the condensates were found in the simulation study to play the central role in controlling the chain length.

We had multiple objectives of optimization in this study; we wished to control the final chain length of polymer product, to maintain a low reaction temperature in each of the three consecutive reactors, to keep P_3 as high as possible, and to reduce the quantity of by-products below the allowable limit. By employing the optimized reaction conditions, we could reduce the energy cost. To have all of these competitive goals satisfied simultaneously, we suggested an objective function F of the following form:

$$F(X_n, T_1, T_2, T_3, P_3, \mathrm{DEG}, \mathrm{Acet}) = \vec{f}^{\,T}\vec{\mathbf{w}} = \begin{bmatrix} f_1(Xn) \\ f_2(T_1) \\ f_3(T_2) \\ f_4(T_3) \\ f_5(P_3) \\ f_6(\mathrm{DEG}) \\ f_7(\mathrm{Acet}) \end{bmatrix}^T \begin{bmatrix} w_1 \\ w_2 \\ w_3 \\ w_4 \\ w_5 \\ w_6 \\ w_7 \end{bmatrix} \tag{59}$$

TABLE VI
Kinetic Parameters for the Reactions in Table IV

k_1	$4.0 \times 10^{4}\exp(-15{,}000/RT)$ L/mol min
k_2	$2.0 \times 10^{4}\exp(-15{,}000/RT)$ L/mol min
k_3	$6.8 \times 10^{5}\exp(-18{,}500/RT)$ L/mol min
k_4	$4.16 \times 10^{7}\exp(-29{,}800/RT)$ min^{-1}
k_5	$4.16 \times 10^{7}\exp(-29{,}800/RT)$ L/mol min
k_6	$4.16 \times 10^{7}\exp(-29{,}800/RT)$ L/mol min
k_7	$1.04 \times 10^{6}\exp(-17{,}600/RT)$ L/mol min
k_8	$1.04 \times 10^{6}\exp(-17{,}600/RT)$ L/mol min
k_9	$3.6 \times 10^{9}\exp(-37{,}800/RT)$ min^{-1}
k_{10}	$6.8 \times 10^{5}\exp(-18{,}500/RT)$ L/mol min
K_1	0.3
K_2	0.15
K_3	0.5
K_7	2.5
K_8	1.25

$R = 1.987$ cal/mol K.

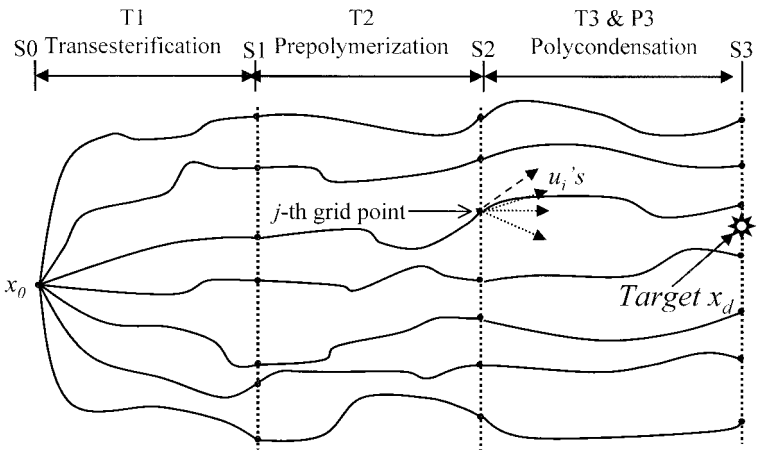

Figure 2 Graphical illustration of the IDP algorithm for the PET process.

in which $\vec{\mathbf{w}}$ is the weighting vector with the weighting factors (w_i) as its components and the f_i's are defined as follows:

$$f_1(Xn) = |Xn_{\text{desired}} - Xn| \tag{60}$$

$$f_i(T_i) = (T_{i-1} - T_{i-1,\text{low}}) \div (T_{i-1,\text{up}} - T_{i-1,\text{low}}), \quad i = 2, 3, 4. \tag{61}$$

$$f_5(P_3) = (P_{\text{up}} - P_3)/(P_{\text{up}} - P_{\text{low}}) \tag{62}$$

$$f_6(\text{DEG}) = \text{DEG}/\text{DEG}_{\text{max}} \tag{63}$$

$$f_7(\text{Acet}) = \text{Acet}/\text{Acet}_{\text{max}} \tag{64}$$

where X_n denotes the number-average degree of polymerization. DEG in eq. (63) is the amount of free DEG and DEG groups in the polymer melt phase at the exit of the third reactor and Acet in eq. (64) is the amount of acetaldehyde in the third reactor. Both DEG_{max} and Acet_{max} were set to 1×10^{-3} mol/L.

We also put constraints on the reaction temperatures of the three consecutive reactors and on the pressure of the polycondensation reactor as follows:

$$170°\text{C} \le T_1 \le 190°\text{C} \tag{65}$$

$$270°\text{C} \le T_2 \le 290°\text{C} \tag{66}$$

$$270°\text{C} \le T_3 \le 290°\text{C} \tag{67}$$

$$0.1 \text{ Torr} \le P_3 \le 1 \text{ Torr}. \tag{68}$$

The number of time intervals was set to three. These were the residence times for each of the transesterification, the prepolymerization, and the polycondensation reactors. With this time span, a grid for the IDP algorithm with constraints was generated. Instead of using a uniform grid, we adopted the procedure suggested by Luus.[13]

First, N allowable values of the control profile in some region r were generated with respect to the control variable u_i (T_1, T_2, T_3, and P_3). Then, integration of the state equations gave N^2 possible trajectories (grid by temperature and pressure). All the states and control variables corresponding to each grid point needed to be saved. Then, optimization started from the third stage (the last stage), according to Bellman's theory.[14] After the first turn of optimization, the obtained best policy, u^{best} ($[T_1\ T_2\ T_3\ P_3]^{\text{best}}$), was set as the initial control profile for the next turn, and the spectra of control regions were reduced by a factor of γ, which was set to 0.8 in this study. In the second turn, a similar procedure was repeated as in the first turn. After each turn, we compared this index with the minimum index of the previous turn and chose the lower one. This procedure is schematically shown in Figure 2 for the scalar case (one control variable). We also enumerate the steps of the algorithm as follows:[9]

1. The system was composed of three successive reactors, and thus, each reactor corresponded to one stage.
2. The number of grid points was set to N per each control variable. During the backward pass, the control u could take on M allowable values inside the control region, r, over which the allowable values of control could be selected.
3. By guessing u^0 for each stage and subsequently perturbing u^0 uniformly inside the allowable region for control, we could select N^2 initial values of control. The number of values of initial control was N^2, N for the temperature multiplied by N for the pressure.
4. With the N^2 control trajectories from step 3, we integrated the state equations to generate and store N^2 values for the grid points at each stage.

TABLE VII
Optimization Strategy when the $X_{ndesired}$ Was Specified as 90 or 95

Weighting vector	w_1 (X_n)	w_2 (T_1)	w_3 (T_2)	w_4 (T_3)	w_5 (P_3)	w_6 (DEG)	w_7 (acetaldehyde)
W0	10	1	1	1	1	0	0
WT2	10	1	100	1	1	0	0
WT3	10	1	1	100	1	0	0
WP3	10	1	1	1	100	0	0
WD	10	1	1	1	1	20	0.2
WDA	10	1	1	1	1	20	20

5. Then, the backward pass started from the last stage, which corresponded to the region from S2 to S3 (see Fig. 2). At each grid point, we integrated the state equations of the third reactor once with each of the M^2 allowable values for u. For each grid point, we chose the value of u that gave the minimum value of the index and stored the value of the control for use in step 6.
6. We stepped back to the second stage, which corresponded to the region from S1 to S2. At each grid point, we integrated the state equations of the second reactor once with each of the M allowable values of control (no control for pressure). To continue integration from S2 to S3, we chose the control from step 5 that corresponded to the nearest grid point. For each grid point, we compared M values of indices and stored the control that gave the minimum value.
7. We repeated this procedure for the first stage, which corresponded to the region from S0 to S1. We stored the control policy that minimized the index.
8. We reduced the region for the allowable control values by a factor of γ so that $r_{next} = \gamma \times r_{present}$. We used the optimal control policy obtained in step 7 as the nominal value for u^0.

We went to step 3 and repeated the procedure for a number of iterations. We compared this optimal index with the previous one and chose the lower index.

SIMULATION RESULTS AND DISCUSSION

Weighting vector

There can be many aspects of trade-off in the production of PET because consumers constantly request polymers with various properties at a reasonable price, and the manufacturers try to meet needs by minimizing costs. One may want to save energy and to operate the process under mild conditions at the expense of quality, or one may want to have good control of the quality of polymer no matter how high the operational cost may be. Therefore, it is necessary to establish an optimization strategy to obtain the desired product.

The energy requirement of the PET process is rather heavy because the reaction temperatures in the prepolymerization and melt polycondensation reactors need to be kept very high, and the pressure of the third reactor needs to be close to vacuum. Manufacturers, however, want to produce polymer with an average chain length larger than 80 using as little energy as possible, that is, keeping the reaction condition as mild as possible. In addition, they simultaneously try to suppress the side reactions that form by-products such as DEG and acetaldehyde.

For this purpose, we propose an objective function incorporating the competitive goals with the predesigned weighting vector according to a production strategy. We consider six different strategies designed to control the quality of polymer product and to minimize production costs. These strategies are denoted as **W0, WT2, WT3, WP3, WD,** and **WDA,** respectively, and the values of the components (w_i's) in each vector are given in Table VII. In every weighting vector, we set w_1 to 10 to obtain the polymer with the desired average chain length with every strategy. For **WT2, WT3,** and **WP3,** which were the strategies aimed at minimizing energy costs, we put a heavier weighting on w_3 in **WT2,** on w_4 in **WT3,** and on w_5 in **WP3,** respectively, to make the optimized reaction temperatures in the second and third reactors as low as possible and the optimized P_3 as high as possible within their respective controllable ranges. The value of w_6 in **WD** was set to 20 so that the amount of free DEG and DEG end groups in the polymer melt phase would be minimized. The values of w_6 and w_7 in **WDA** were set to 20 so that both the amount of free DEG and DEG end groups in the polymer melt phase and the amount of acetaldehyde condensate would be minimized.

Average chain length

For each of the various strategies, we conducted a simulation study for optimization to examine whether the average chain length approached the desired value, which was specified as 90 or 95 in this study. The final chain length reached the desired value in every case within less than 1.3 % of the relative error.

As shown in Figures 3 and 4, in the case of **W0,** to obtain a polymer with a larger molecular weight, we did not need to keep T_1 and T_2 higher, but rather P_3 and T_3 were found to play the central roles. In other words, to increase the polymer chain length, it was more important to remove condensates such as EG, MeOH, and water by keeping P_3 very low.

According to Renwen et al.[15] and Laubriet et al.,[10] DEG content decreases at high temperatures and low pressures. In the cases of **WD** and **WDA,** as shown in Figure 4, P_3 reached the lower bound (0.1 Torr) to decrease the amount of by-products, but T_3 was not higher than those in other cases. We believe that T_3 was not increased further because an increase in T_3 brought about a higher energy cost.

Reaction conditions

When the **W0** strategy was applied, both T_1 and T_2 as shown in Figure 3(a), were higher than those shown in Figure 3(b). On the contrary, P_3 as shown in Figure 4(b) was lower than that shown in Figure 4(a), although the T_3's as shown in Figures 4(a) and 4(b) were similar. Therefore, the reaction condition in the last reactor exercised a dominant influence on the polymer property, which was represented by the average chain length in this work.

When the **WT2** strategy was applied, T_2 was lower by more than 10°, and T_3 was also lower by about 5° in comparison to the results for the case of **W0,** as shown in Figures 3(a) and 4(a). The lowered T_2 resulted in a prepolymer with a shorter average chain length. Thus, by keeping either T_3 higher or P_3 lower, we obtained the polymer with desired chain length at the exit of the melt polycondensation reactor. As shown in Figures 3(b) and 4(b), however, the differences in T_2 and T_3 between the two cases of **W0** and **WT2** were not so big. As shown in Figure 4, P_3's reached the lower bound, whereas T_3 was lower than or the same as T_3 in the case of **W0** because lowering P_3 was more influential than raising T_3 when minimizing the value of the objective function with the **WT2** strategy.

If we compare the two strategies, **WT3** and **WT2**, T_2 in the case of **WT3** was higher, whereas T_3 did not decrease. The increase in T_2 resulted in an increase in the average chain length of the prepolymer, and thus, P_3 was a littler higher than that for the **WT2** strategy, as shown in Figure 4.

The most interesting result appeared when we applied the **WP3** strategy. As expected, P_3's as shown in Figure 4(a) and 4(b) were higher by 0.28 and 0.2 Torr, respectively, in comparison to the results of the **W0** strategy. At the same time, all of T_1, T_2, and T_3 values needed to be kept high so that the polymer with the desired average chain length could be obtained (see Figs. 3 and 4). When the **WP3** strategy was applied, we obtained the largest amount for each of DEG, carboxylic acid groups, unsaturated vinyl groups in the polymer melt phase, and acetaldehyde condensate under the mildest condition of P_3. The amounts of DEG (free DEG + DEG end groups), carboxylic acid groups, and unsaturated vinyl groups in the polymer melt phase were in the order of 10^{-3}–10^{-2} g/g of mixture, 10^{-6} mol/g of mixture, and 10^{-6} mol/g of mixture, respectively, and these were compatible with the results of Laubriet et al.[10] in terms of the order of magnitude.

As mentioned previously, when the **WD** and **WDA** strategies were applied, the optimized P_3 was determined at its lower bound. Figures 5, 6, and 7 show that the contents of EG, water, carboxylic acid groups, and unsaturated vinyl group as well as those of DEG and acetaldehyde increased or decreased according to the variations of T_2 and P_3 presented in Figures 3 and 4. According to Ravindranath and Mashelkar,[2] the increased reactor temperature (T_2) in the prepolymerization reactor appeared to be responsible for the enhancement of the formation of DEG, acetaldehyde, carboxylic acid groups, and water.

CONCLUSIONS

The constrained IDP algorithm was successfully applied to the entire PET process to control the final chain length of the PET product, to lower the energy consumption directly related to the reaction conditions, and to suppress side reactions. By conducting the optimization, we obtained a recipe to produce the polymer product with desired qualities and enhanced the reactor performance. Using six different sets of weighting vectors, we introduced an optimization strategy to obtain the desired polymer product. The highly nonlinear behavior of the process of our concern was not an obstacle to the optimization scheme because the IDP algorithm could find the optimized reaction conditions by examining all the possible pathways within the allowable control regions.

As shown in Figure 8, X_n reached the desired value in every case within less than 1.3 % of the relative error. The reaction temperatures were not always high, although the desired chain length was set to a high value. Instead, keeping T_1 and T_2 higher brought about larger amounts of condensates, including by-products in the reaction media, which made it much more difficult to raise the polymer chain length and to suppress the side reactions in the subsequent reactors. P_3 played a central role in increasing the average chain length. If a higher chain length is to be obtained, P_3 is required to be lower according to the model predictions and the IDP algorithm. In addition, if the side reactions should be suppressed, P_3 is also found to take an important role. In the cases of the **WD** and **WDA** strategies, the optimized pressure was at the lower bound, whereas the temperature was not higher than those in other cases. Also, the contents of EG,

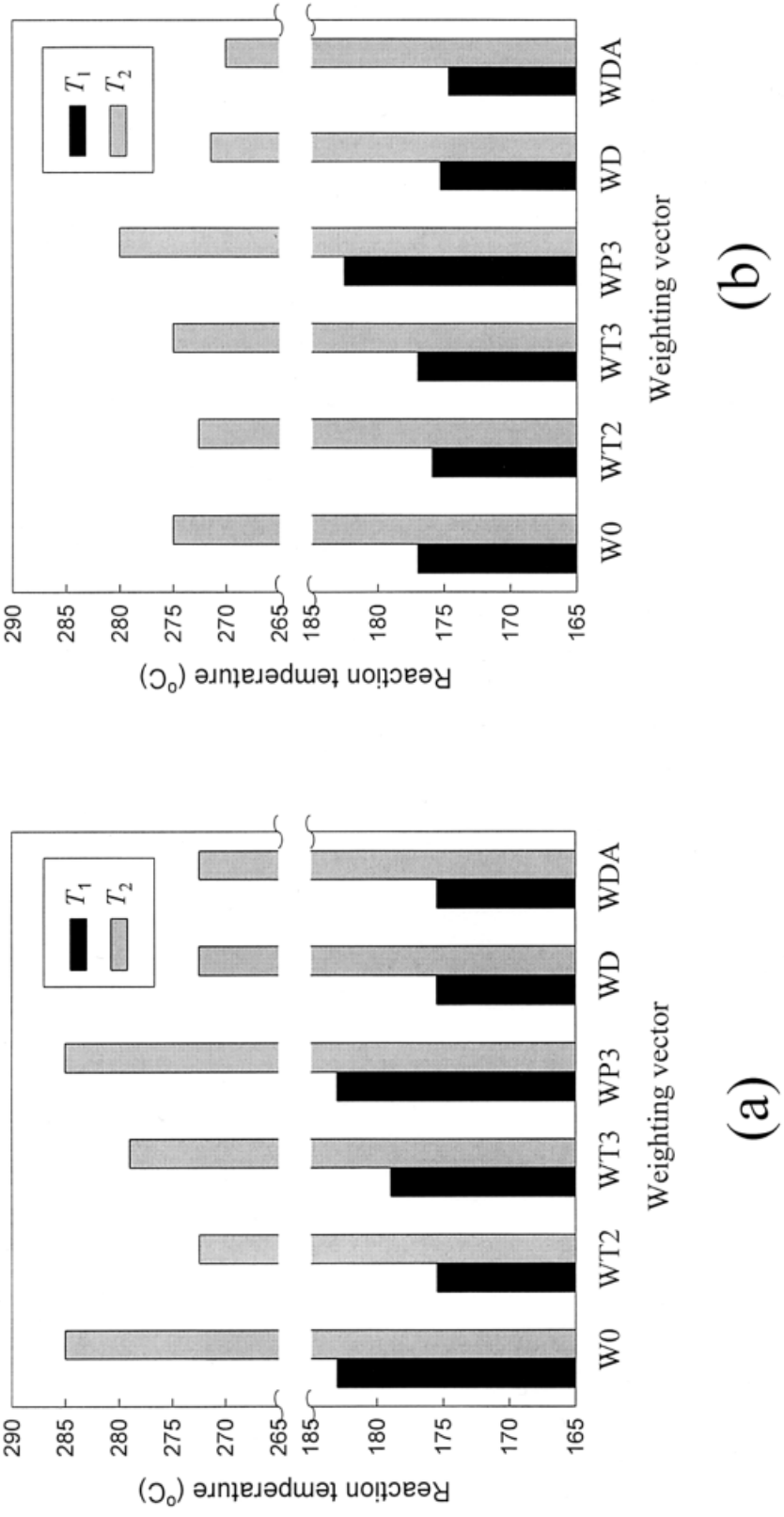

Figure 3 Optimized reaction temperatures in the transesterification and prepolymerizaion reactors according to the six different optimization strategies when $X_{n\ \text{desired}}$ was (a) 90 and (b) 95.

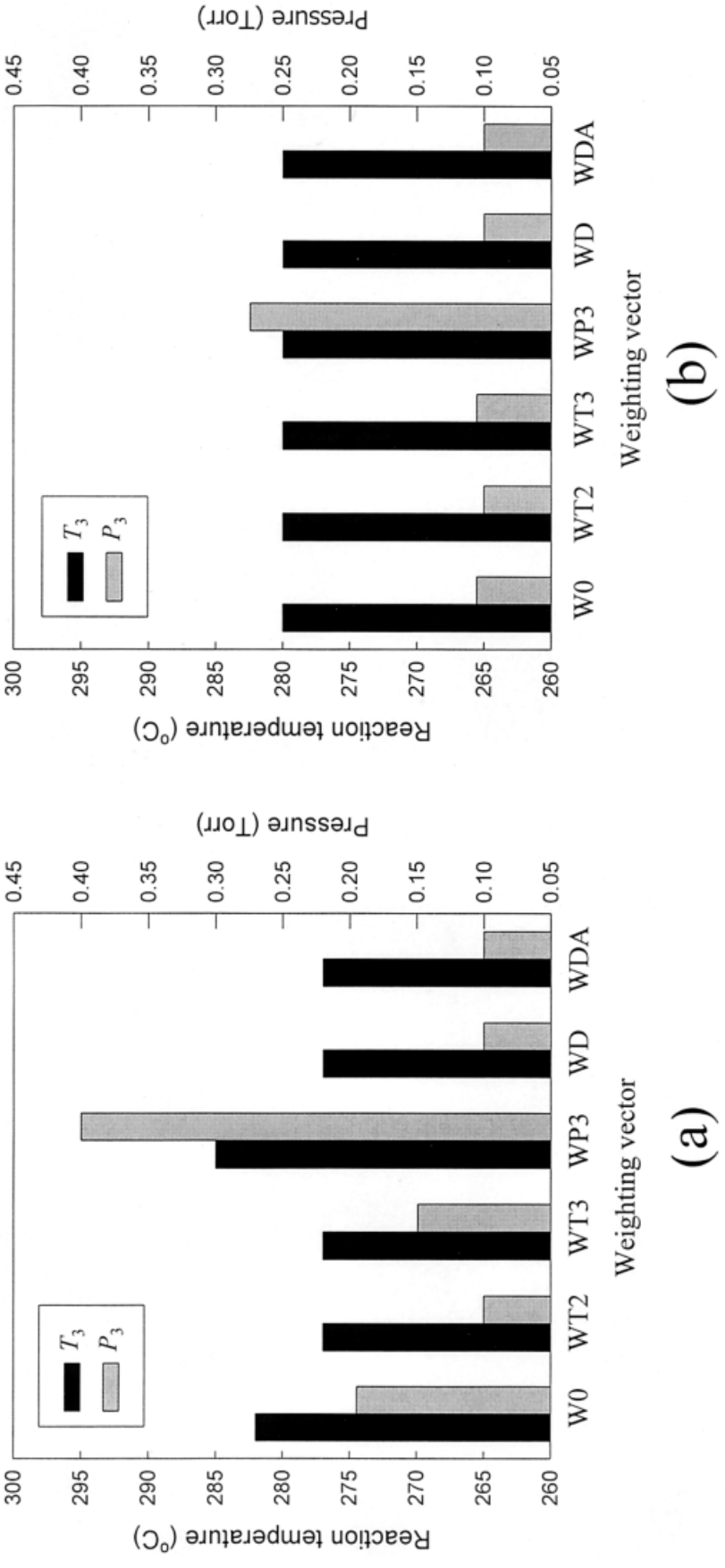

Figure 4 Optimized reaction temperature (T_3) and pressure (P_3) in the melt polycondensation reactor according to the six different optimization strategies when $X_{n\ \mathrm{desired}}$ was (a) 90 and (b) 95.

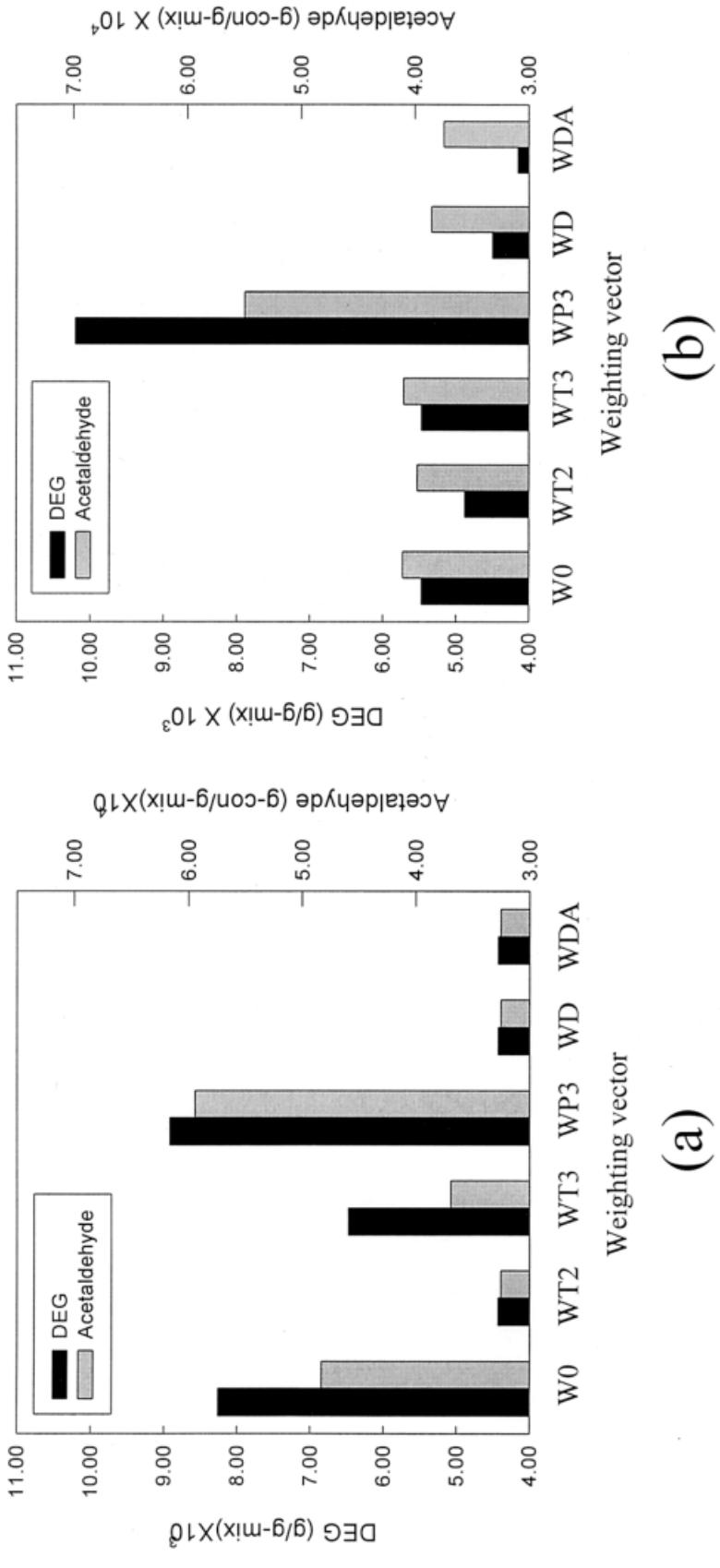

Figure 5 Contents of DEG in the polymer melt phase and acetaldehyde produced in the melt polycondensation reactor according to the six different optimization strategies when $X_{n\ \text{desired}}$ was (a) 90 and (b) 95.

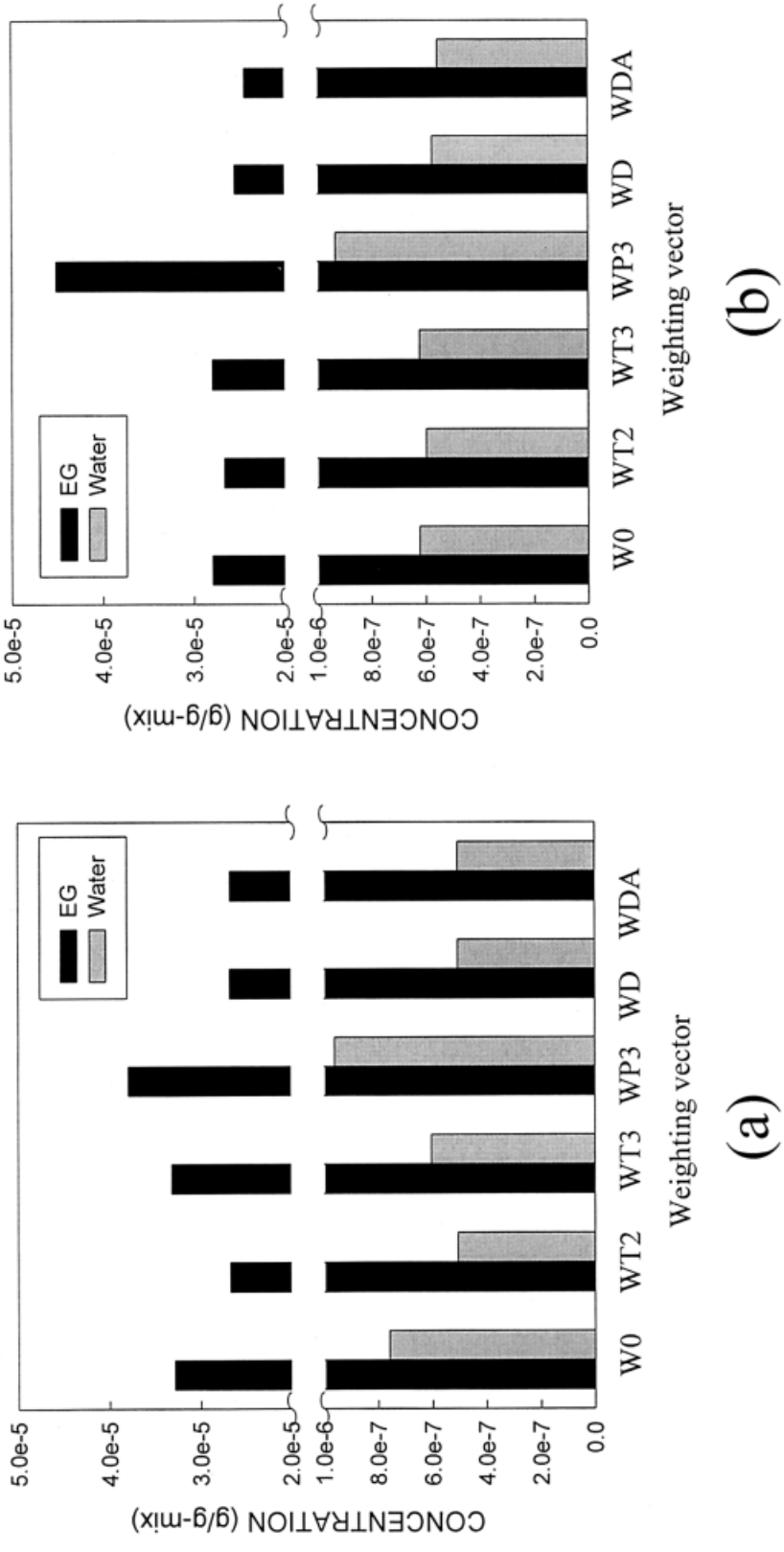

Figure 6 Contents of EG and water in the polymer melt phase of the melt polycondensation reactor according to the six different optimization strategies when $X_{n\ \text{desired}}$ was (a) 90 and (b) 95.

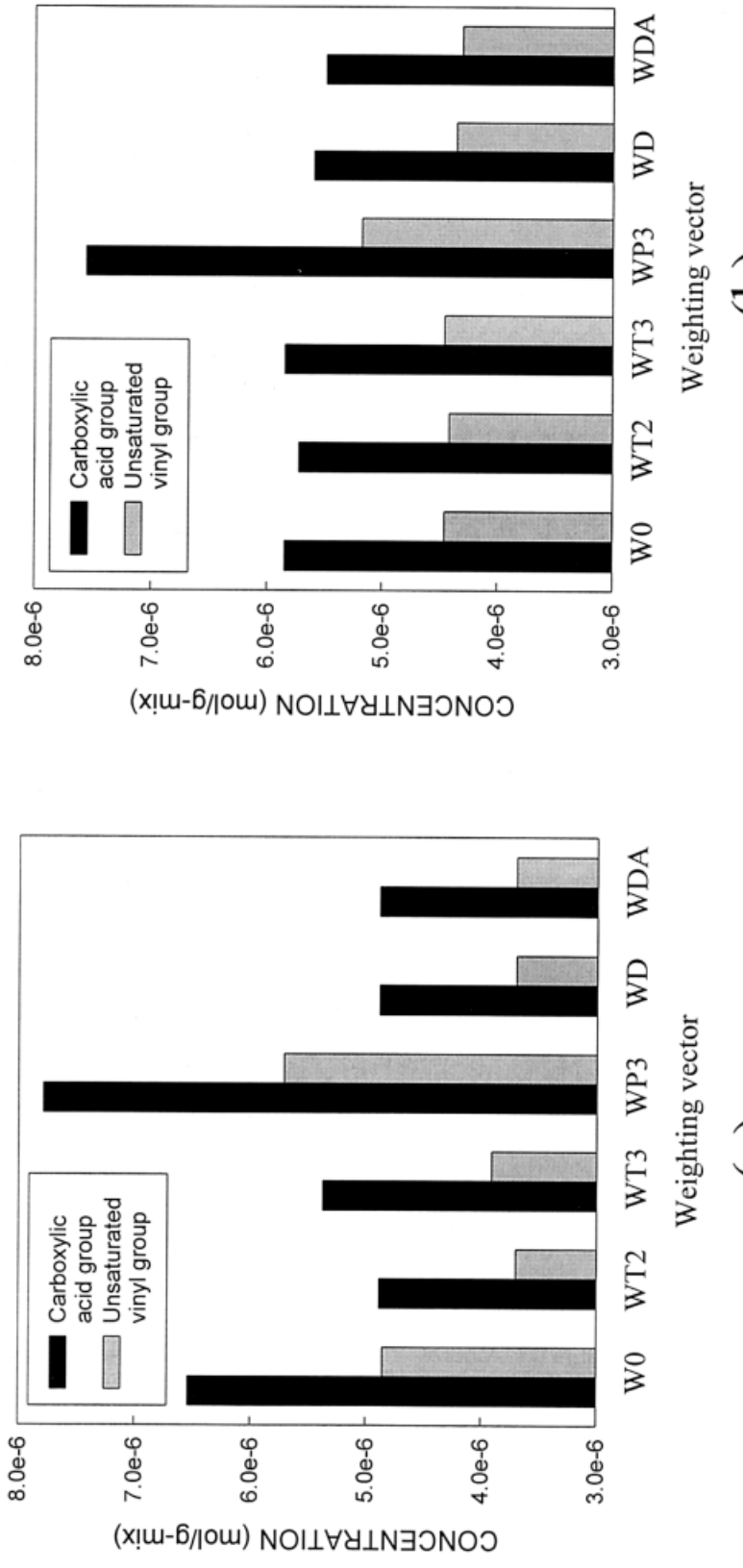

Figure 7 Contents of the carboxylic acid group and the unsaturated vinyl group in the polymer melt phase of the melt polycondensation reactor according to the six different optimization strategies when $X_{n\ \text{desired}}$ was (a) 90 and (b) 95.

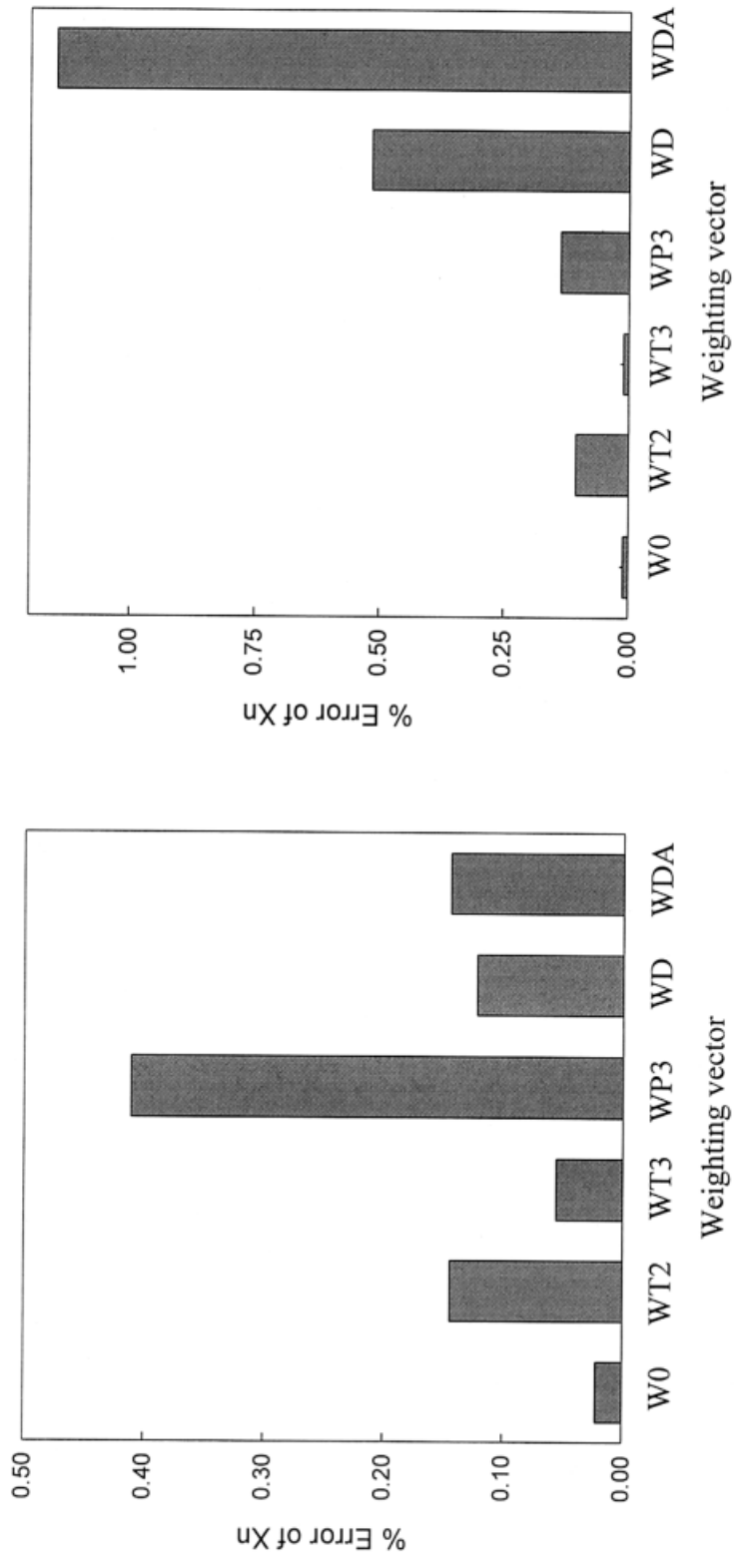

Figure 8 Relative errors between X_n and $X_{n\ \text{desired}}$ according to the six different optimization strategies when $X_{n\ \text{desired}}$ was (a) 90 and (b) 95.

water, carboxylic acid groups, and unsaturated vinyl groups as well as those of DEG and acetaldehyde were mainly affected by variations of T_2 and P_3.

An optimized recipe cannot be provided simply by superposing the separately optimized reaction conditions for individual stages but can be provided by optimizing the reaction conditions for the entire process at the same time.

References

1. Ravindranath, K.; Mashelkar, R. A. J Appl Polym Sci 1982, 27, 471.
2. Ravindranath, K.; Mashelkar, R. A. Polym Eng Sci 1982, 22, 619.
3. Ravindranath, K.; Mashelkar, R. A. AIChE J 1984, 30, 415.
4. Ravindranath, K.; Mashelkar, R. A. Chem Eng Sci 1986, 41, 2969.
5. Lei, G. D.; Choi, K. Y. J Appl Polym Sci 1990, 41, 2987.
6. Lei, G. D.; Choi, K. Y. Ind Eng Chem Res 1992, 31, 769.
7. Ravindranath, K.; Mashelkar, R. A. Chem Eng Sci 1986, 41, 2197.
8. Patwardhan, A. A.; Rawlings, J. B.; Edgar, T. F. Chem Eng Commun 1990, 87, 123.
9. Dadebo, S. A.; Mcauley, K. B. Comput Chem Eng 1995, 19, 513.
10. Laubriet, C.; LeCorre, B.; Choi, K. Y. Ind Eng Chem Res 1991, 30, 2.
11. Tai, K.; Arai, Y.; Teranishi, H.; Tagawa, T. J Appl Polym Sci 1980, 25, 1789.
12. Rafler, G.; Bonatz, E.; Sparing, H. D.; Otto, B. Acta Polym 1987, 38, 6.
13. Luus, R. Optimal Control by Dynamic Programming Using Accessible Grid Points and Region Contraction. Hung J Ind Chem 1989, 17, 523.
14. Bellamn, R. Dynamic Programming; Princeton University Press: Princeton, NJ, 1957.
15. Renwen, H.; Feng, Y; Tinzheng, H.; Shiming, G. Angew Makromol Chem 1983, 119, 159.